

Long-Time Non-Contact Water Level Measurement with a 5.8-GHz DC-Coupled Interferometry Radar

Zhengyu Peng¹, Ashish Mishra¹, Justin R. Davis², Jennifer A. Bridge², Changzhi Li¹

¹Department of Electrical & Computer Engineering, Texas Tech University Lubbock, Texas

²Department of Civil & Coastal Engineering, University of Florida, Gainesville, Florida
zhengyu.peng@ttu.edu

Abstract—Flooding caused by tropical cyclones, tsunami, and many other phenomena is one type of natural disaster that occurs all around the world. While these disasters cannot be prevented, the communities can be made more resilient and damages caused by them to lives and infrastructure can be minimized by developing early warning systems. Microwave-based systems provide a non-contact measurement setup to monitor water level, thus requiring low maintenance and operation costs. In this paper, a DC-coupled 5.8-GHz interferometry radar was designed and tested by observing water level in a barrel, which had water poured in and drained out over a long-time period. By adding more gains to the RF chain and removing the gain in the baseband, the proposed water-level monitoring radar system eliminates the requirement of complex DC tuning structure in the previous works. The experiment demonstrated that the proposed water-level monitoring radar system was able to accurately measure the relative position of water with mm-accuracy.

Keywords—Interferometry radar, dc-coupled, displacement measurement, large displacement, water-level

I. INTRODUCTION

Recently, there has been large-scale research on developing reliable and accurate systems to monitor flooding from natural disasters, such as tropical cyclones, and tsunami, etc. These natural disasters cause large-scale loss-of-life and destruction of infrastructure. Although some events cannot be prevented, early warning systems can be used to warn people and minimize the damage caused by them. In this paper, a novel method to monitor water level is discussed. This system can be used to monitor the rising water level to warn about a potential flood and the status of receding water level after a flood. Additionally, for wind-driven flooding events, it can be used to measure wave heights.

There has been a lot of research in designing water monitoring systems. Many methods are available to measure water level or to indicate flood water. Some of these methods utilize the color of water to differentiate flood water from normal water [1], but this kind of system can be affected by human and animal activities. Also, this might not provide accurate reading during night or foggy conditions. The pressure transducers as discussed in [2] require specialized hardware setup and this equipment may be swept away or get damaged under heavy water flow. The use of buoys [3], [4] for measuring the water level requires sophisticated instruments and buoys are not

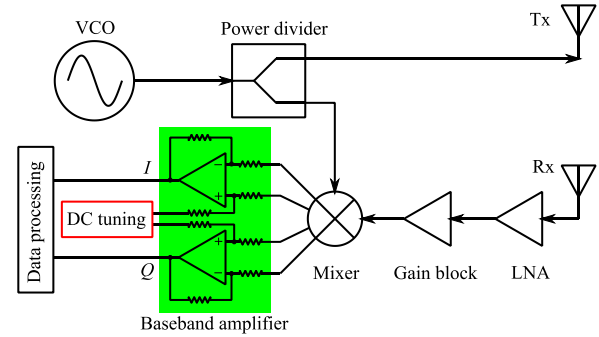


Fig.1. Block diagram of the interferometry radar with DC tuning for water level monitoring [7].

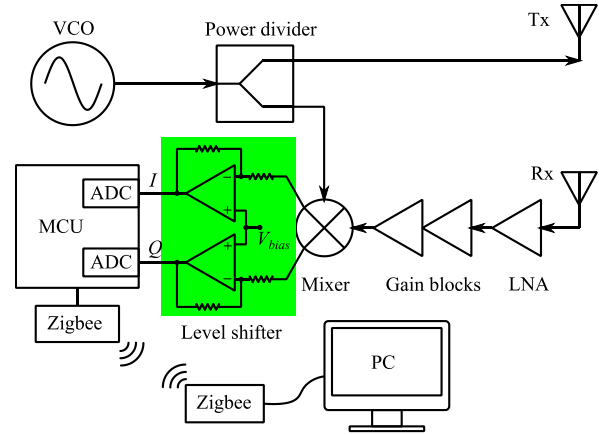


Fig. 2. Block diagram of the proposed interferometry radar based water level monitoring system.

suitable for rough conditions. Moreover, the tilts in buoys during measurement can cause errors. The use of cameras to capture an image of a staff gauge and image processing technique to estimate the level of water [5] cannot work during low visibility conditions. These contact methods of water measurement also degrade fast due to constant corrosion and biofouling.

Microwave systems, which provide an inexpensive and effective non-contact method to measure water levels, are not affected by weather and visibility conditions. Due to its non-contact measurement feature, their risks of corrosion or biofouling are minimized. Range radars, such as FMCW radars and pulsed radars, can be used to measurement the absolute

distance between the target and the radar. However, FMCW radars demands a large signal bandwidth and pulsed radars lack necessary accuracy [6]. Interferometry radar is one of the most effective and low-cost systems to measure high sensitivity motion with mm-accuracy. An interferometry radar has been used to successfully monitor the change of water levels [7]. However, as shown in Fig. 1, a complex DC tuning structure was required to compensate the DC offsets introduced by T/R leakage and reflections from stationary clutters. In addition, the DC offsets need to be continuously calibrated during the measurement, which makes the baseband signal processing complicated.

In this paper, a 5.8-GHz interferometry radar is used to monitoring the change of water levels in a barrel. Compared with the previous work [7], the proposed DC-coupled 5.8-GHz interferometry radar has more gain in the RF domain in the receiver chain. In the baseband, a level shifter is used to make sure the baseband signals are in the voltage range of the analog-to-digital convertors (ADCs). With this configuration, the proposed interferometry radar alleviates the need of dynamical DC tuning structure and algorithm. Two-channel ADCs from a micro-controller are used to sample the baseband data. The digital data is transmitted through Zigbee and recorded by a computer. A 10.5-hour long-term experiment has been taken to evaluate the capability of the proposed water-level monitoring interferometry radar. During the experiment, a barrel was filled and drained at varying time intervals. The arctangent demodulation was utilized to calculate the change of water levels during the monitoring period. Compared with the measuring tape, the proposed interferometry radar can accurately monitor the change of water levels in a long time.

The paper is divided into four sections. Section II outlines the theory. Section III discusses the measurement setup and the results. Conclusions are drawn in Section IV.

II. THEORY AND RADAR DESIGN

A. Theory

As shown in Fig. 2, the general architecture of an interferometry radar contains a single tone generator (i.e., an oscillator), a pair of antennas, several stages of amplifiers, a mixer, a low-pass filter (LPF) and a baseband processing unit.

The single tone signal generated by the oscillator can be expressed as:

$$S_t(t) = \cos(2\pi f_c t + \phi(t)) \quad (1)$$

where f_c is the frequency and $\phi(t)$ is the phase noise.

The received signal $S_r(t)$ is:

$$S_r(t) = \cos\left(2\pi f_c t - \frac{4\pi x(t)}{\lambda} - \phi\left(t - \frac{2x_o}{c}\right)\right) \quad (2)$$

where c is the speed of light. $x(t)$ is the change of water level due to leakage or filling in the barrel. λ is free space wavelength.

The baseband signal $B(t)$ is the low-pass filtered portion of the product of the received signal $S_r(t)$ and a copy of the transmitted signal $S_t(t)$:

$$B(t) = \cos\left(\frac{4\pi x(t)}{\lambda} + \Delta\phi(t)\right) \quad (3)$$

where $\Delta\phi(t)$ is the residual phase noise from the oscillator, which can be neglected in the coherent interferometry radar.

A quadrature mixer is necessary to solve the issue of null detection points [8]. In-phase (I) and quadrature (Q) baseband signals can be obtained.

$$B_I(t) = A_I \cos\left(\frac{4\pi x(t)}{\lambda}\right) + V_{DC} \quad (4)$$

$$B_Q(t) = A_Q \sin\left(\frac{4\pi x(t)}{\lambda}\right) + V_{DC} \quad (5)$$

where A_I and A_Q are the amplitudes of I and Q channels. V_{DC} is the DC offset.

After removing the DC offset and normalizing A_I and A_Q amplitudes, (4) and (5) can be converted to (6) and (7) respectively.

$$B'_I(t) = \cos\left(\frac{4\pi x(t)}{\lambda}\right) \quad (6)$$

$$B'_Q(t) = \sin\left(\frac{4\pi x(t)}{\lambda}\right) \quad (7)$$

Small angle approximation can be applied only to small displacements. For practical applications, nonlinear demodulation approach is considered more precise to recover the full phase information [9]. Arctangent demodulation is one of the most widely used method for nonlinear demodulation [9]. By using the arctangent demodulation, water displacement $x(t)$ can be easily calculated:

$$\begin{aligned} x(t) &= \frac{\lambda}{4\pi} \left(\arctan\left(\frac{B'_Q(t)}{B'_I(t)}\right) + k\pi \right) \\ &= \frac{\lambda}{4\pi} \left(\arctan\left(\frac{\sin\left(\frac{4\pi x(t)}{\lambda}\right)}{\cos\left(\frac{4\pi x(t)}{\lambda}\right)}\right) + k\pi \right) \end{aligned} \quad (8)$$

where $k\pi$ is phase unwrapping term, which is used to solve the discontinuity when the demodulation exceeds the range of $(-\pi/2, \pi/2)$.

Based on (3), it may be implied that phase modulation is inversely proportional to the carrier wavelength, so higher frequency will lead to better sensitivity in detection by

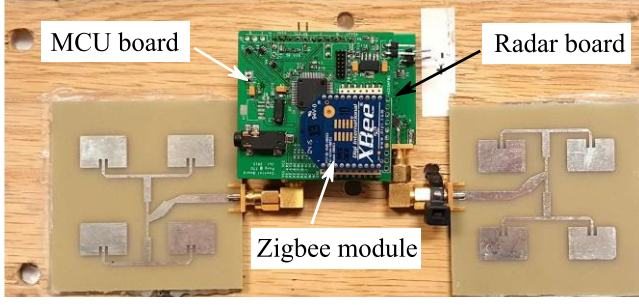


Fig. 3. Photo of the 5.8-GHz interferometry radar.

TABLE I. MAIN COMPONENTS USED IN THE 5.8-GHz INTERFEROMETRY RADAR

Part	Part number	Manufactory
VCO	HMC358MS8G	Analog Devices
Power Divider	GP2X1	Mini-Circuits
LNA	HMC320MS8G	Analog Devices
Gain Block	NBB 400	Qorvo
Mixer	HMC525LC4	Analog Devices
Baseband Amplifier	ADA4581	Analog Devices
Zigbee	XBee	Digi
Microcontroller	MSP430	Texas Instruments

producing more phase shift for the same amount of motion [10], [11]. However, shorter wavelength is more vulnerable to phase ambiguity. Higher carrier frequency implies shorter phase unambiguous range. For a 2.4-GHz interferometry radar, unambiguous range is 6.25cm, and a 5.8-GHz interferometry radar has the unambiguous range of 2.58cm. For example, if water level changes more than $\lambda/2$ between two samples, the radar cannot provide reliable measurement results without extra phase unwrapping steps. As a result, there is a tradeoff between sensitivity and unambiguous range.

B. Radar Design

In the previous work, as shown in Fig. 1, the gain in the receiver chain was allocated both in the RF domain and the baseband domain. It is known that the output of the mixer has DC offset, which is introduced by T/R leakage and reflections from stationary clutters. When the DC offset is amplified with the baseband signal by the baseband amplifier, the baseband signal could be easily out of the output voltage range if the bias of the amplifier is not set correctly. Since the DC offset is sensitivity to the environment, it is necessary to continuously tune the bias of the amplifier to guarantee the baseband signal is always in the output voltage range [7]. This dynamic DC tuning leads to extra hardware, control algorithm, and power consumption.

To eliminate the requirement of dynamic DC tuning, in the proposed radar system shown in Fig. 2, all the receiver gain is allocated in the RF domain before the mixer. In this case, the DC offset from the output of the mixer will not be further amplified. Thus, it is possible to set an appropriate DC offset that does not need to be tuned in real time, and ensure the baseband signal is within the dynamic range of the ADC.

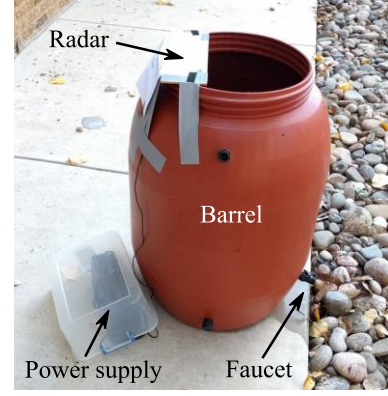


Fig. 4. Photo of the experimental setup.

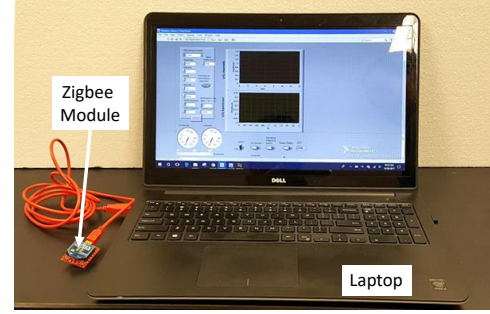


Fig. 5. Photo of the Zigbee receiver and signal processing laptop.

III. EXPERIMENTAL SETUP AND RESULTS

The block diagram of the proposed water level monitoring 5.8-GHz interferometry radar is illustrated in Fig. 2. A 5.8-GHz single tone is generated by a voltage-controlled oscillator (VCO) at power level of 11 dBm. This single tone signal is divided into two paths. One path is connected to the transmitting antenna, which has 11.8 dB gain. The other path serves as a local oscillator (LO) for the mixer. A MSP430 micro-controller was used to sample the baseband data and sent out the data wirelessly through a Zigbee module. The antennas used in the radar system is a pair of 2×2 patch arrays, which have the gain of 11.8 dB. The half-power beam width of the antennas is 46° . In the experiment, the change of the water level was controlled in a very slow rate, thus, 20 samples per second sampling rate for the baseband signals is enough.

The photo of the 5.8-GHz interferometry radar is shown in Fig. 3. Main components used in the radar are listed in Table I. Fig. 4 shows the experimental setup of water level monitoring. The radar, which was powered by an uninterruptible power supply (UPS), was mounted on the top of the barrel. The barrel was filled twice until full. Then, the faucet at the bottom of the barrel was open to drain the water. The draining speed was adjusted during the experiment, and the experiment was carried out for 10.5 hours. A laptop connected with a Zigbee coordinator was used to receive and recode the data.

Figure 6 is the time domain voltages, $B_I(t)$ and $B_Q(t)$, for the I/Q channels. During the 0 - 0.4 hours and the 1.63 - 1.75 hours, water was poured into the barrel with a smaller container.

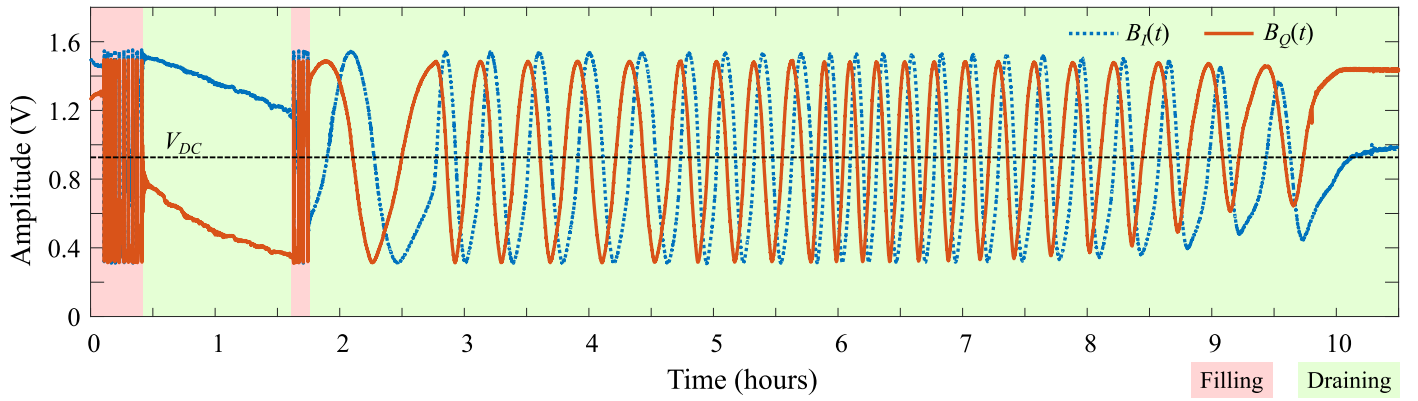


Fig. 6. Time domain signals of I/Q channels.

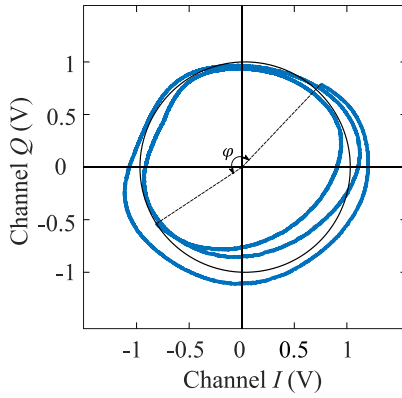


Fig. 7. Normalized constellation graph for 8 to 9 hours of measurement.

Between the 0.4 and 1.63 hours water was leaking very slowly. Starting from 1.75 hours, the water was made to leak from the barrel at a higher rate till 2.8 hours. The water leakage rate was manually increased at 2.8 hours, 4.73 hours and 5.76 hours.

Figure 7 shows the normalized constellation graph obtained for the 8 to 9 hours of measurement, when water leaked from the barrel. The constellation graph makes one complete cycle for every $\lambda/2$ change in the water level. For a 5.8-GHz interferometry radar, the constellation graph makes a complete cycle for every 2.58 cm change in water level. The displacement measurement from the constellation graph can be calculated as

$$d = \frac{\lambda}{2}n + \frac{\lambda\varphi}{4\pi} \quad (10)$$

where, n denotes the number of complete circles. φ is the angle between the start and end of the trace. During the time duration in Fig. 7, the curve makes two complete circles and an angle φ between the start and end of the curve. By accumulating the total angle in the constellation graph, the change of the water level can be obtained. It should be noted that the curve in Fig. 7 is not perfectly circular due to mismatch between the I and Q channels and multipath reflections. However, the imperfectness doesn't affect the accuracy of the measurement.

Figure 8 gives a clear picture of the water level profile in the barrel from the beginning to 10.5 hour. The rise in the curve signifies filling of water, the constant horizontal line indicates

that the water was neither leaking nor barrel was filled, while the decreasing curve signifies the leakage of water. The slope of the curve signifies the rate at which water was being added for case of positive slope of Fig. 8. The negative slope gives information about the rate of leakage. The positive slopes were very large which means that water was filled rapidly to the barrel. The leakage side showed variable slopes that signifies the different leakage speed of the water from barrel. The changes of the slopes are clearly seen at 2.8 hours, 4.73 hours and 5.76 hours, when the water leakage speed was adjusted. After 7 hours, since the water pressure was reducing, the water flow automatically got reduced. At 9.75 hours of measurement, the water in the barrel got almost empty. The total change in water level is 0.6 m, which is the same as the measured level by a tape.

Figure 9 shows an instance of the water flow profile from 1.6 hours to 1.8 hours. In this period, water was filled into the barrel by a smaller container, which can be seen in Fig. 4. A stair shape can be clearly observed. Each jump in the curve implies filling one container of water. Ripples are also observed at the end of each water level jump. These ripples reflect the unstable water surface after water filling by a container. In addition, stronger ripples can be seen at lower water level, which means the disturbance of water surface by filling water is stronger when the water level is lower.

The water-level change rate curve is illustrated in Fig. 10. The instances, where the leakage rate of water was adjusted, show sudden drops on the rate at 2.8 hours, 4.73 hours and 5.76 hours. The decreasing in leakage can be clear seen from 6 hours to 9 hours as the water pressure was decreasing.

IV. CONCLUSION

In this paper, a 5.8-GHz interferometry radar was used to monitoring the change of water levels in a barrel. Different from a previous work, the proposed DC-coupled 5.8-GHz interferometry radar no longer required a DC tuning structure. This was achieved by adding more gain in the RF domain and removing the gain in the baseband. Two-channel ADCs from a micro-controller were used to sample the baseband data. The digital data was transmitted through Zigbee and recorded by a computer. A 10.5 hours long time experiment had been taken to

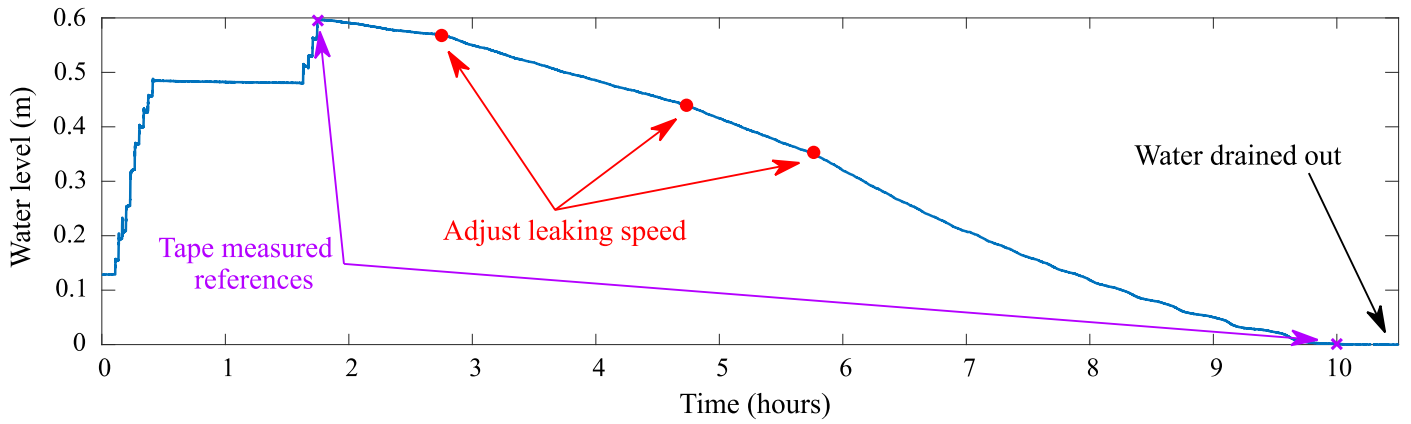


Fig. 8. Demodulated data.

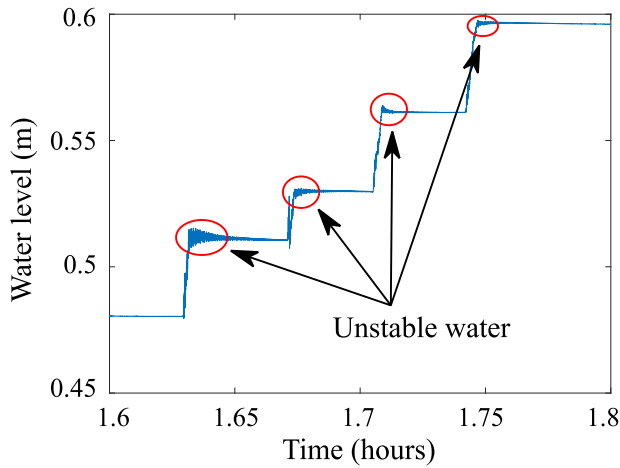


Fig. 9. Water flow profile for 1.6 to 1.8 hour.

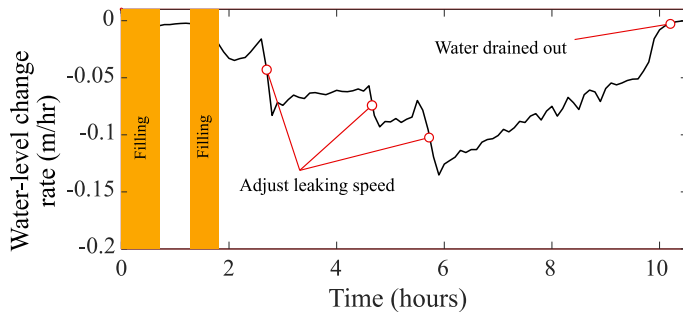


Fig.10. Water-level change rate.

evaluate the capability of the proposed water-level monitoring interferometry radar. This work proved that DC-coupling architecture can achieve high water level measurement accuracy during long-term operation. Future works will be focused on performing this experiment in realistic environment for a longer period of time and under various weather conditions, such as rain and strong wind.

ACKNOWLEDGMENT

The authors would like to acknowledge grant support from National Science Foundation (NSF) ECCS-1760497.

REFERENCES

- [1] O. Intharasombat and P. Khoenkaw, "A low-cost flash flood monitoring system," in *7th International Conference on Information Technology and Electrical Engineering (ICITEE)*, Chiang Mai, 2015, pp. 476-479.
- [2] E. Yuliza, R. A. Salam, I. Amri, E. D. Atmajati, D. A. Hapidin, I. Meilano, M. M. Munir, and M. Abdullah, "Characterization of a water level measurement system developed using a commercial submersible pressure transducer," in *International Conference on Instrumentation, Control and Automation (ICA)*, Bandung, 2016, pp. 99-102.
- [3] R. Heitsenrether, W. Hensley, W. Krug and E. Breuer, "Development of a standalone real-time water level measurement system to support safe navigation along Alaska's arctic coasts," in *OCEANS*, Washington, DC, 2015, pp. 1-8.
- [4] S. H. M. Ngagipar and O. M. Yusof, "RTK GPS water level measurement on dynamic sea surface," in *IEEE Control and System Graduate Research Colloquium*, Shah Alam, 2011, pp. 82-85.
- [5] M. Bruinink, A. Chandarr, M. Rudinac, P. J. van Overloop and P. Jonker, "Portable, automatic water level estimation using mobile phone cameras," in *14th IAPR International Conference on Machine Vision Applications (MVA)*, Tokyo, 2015, pp. 426-429.
- [6] P. Gulden, M. Vossiek, M. Pichler and A. Stelzer, "Application of State-Space Frequency Estimation to a 24-GHz FMCW Tank Level Gauging System," in *33rd European Microwave Conference*, Munich, Germany, 2003, pp. 995-998.
- [7] C. Gu, W. Xu, G. Wang, T. Inoue, J. A. Rice, L. Ran, and C. Li, "Noncontact Large-Scale Displacement Tracking: Doppler Radar for Water Level Gauging," *IEEE Microwave and Wireless Components Letters*, vol. 24, no. 12, pp. 899-901, Dec. 2014.
- [8] M. Mercuri, Y. H. Liu, I. Lorato, T. Torfs, A. Bourdoux and C. Van Hoof, "Frequency-Tracking CW Doppler Radar Solving Small-Angle Approximation and Null Point Issues in Non-Contact Vital Signs Monitoring," *IEEE Transactions on Biomedical Circuits and Systems*, vol. 11, no. 3, pp. 671-680, June 2017.
- [9] B. K. Park, O. Boric-Lubecke and V. M. Lubecke, "Arctangent Demodulation With DC Offset Compensation in Quadrature Doppler Radar Receiver Systems," *IEEE Transactions on Microwave Theory and Techniques*, vol. 55, no. 5, pp. 1073-1079, May 2007.
- [10] C. Gu, "Short-Range Noncontact Sensors for Healthcare and Other Emerging Applications: A Review," *Sensors*, vol. 16, no. 8, p.1169, Jul. 2016.
- [11] C. Gu, T. Inoue and C. Li, "Analysis and Experiment on the Modulation Sensitivity of Doppler Radar Vibration Measurement," *IEEE Microwave and Wireless Components Letters*, vol. 23, no. 10, pp. 566-568, Oct. 2013.